Palaeogeography, Palaeoclimatology, Palaeoecology 295 (2010) 215–225

Contents lists available at ScienceDirect

Palaeogeography, Palaeoclimatology, Palaeoecology

journal homepage: www.elsevier.com/locate/palaeo

Fast or slow melting of the Marinoan snowball Earth? The cap dolostone record

E. Font [a,*], A. Nédélec [b], R.I.F. Trindade [c], C. Moreau [d]

[a] IDL, Faculdade de Ciências da Universidade de Lisboa, Campo Grande, 1749-016, Lisboa, Portugal
[b] LMTG, UMR 5563, Université de Toulouse – CNRS-IRD, OMP, 14 avenue Edouard-Belin, 31400 Toulouse, France
[c] Instituto de Astronomia, Geofísica e Ciências Atmosféricas, Universidade de São Paulo, São Paulo, Brazil
[d] CEA/Saclay, LMC14 – UMS2572, Bât. 450 – Pte 4E, 91191 Gif-sur-Yvette Cedex, France

ARTICLE INFO

Article history:
Received 5 July 2009
Received in revised form 28 April 2010
Accepted 28 May 2010
Available online 4 June 2010

Keywords:
Neoproterozoic
Marinoan glaciation
Snowball Earth
Cap dolostone
Magnetostratigraphy
Microbially-mediated dolomite precipitation
Carbon cycle

ABSTRACT

The end of the Neoproterozoic era is punctuated by two global glacial events marked by the presence of glacial deposits overlaid by cap carbonates. Duration of glacial intervals is now consistently constrained to 3–12 million years but the duration of the post-glacial transition is more controversial due to the uncertainty in cap dolostone sedimentation rates. Indeed, the presence of several stratabound magnetic reversals in Brazilian cap dolostones recently questioned the short sedimentation duration (a few thousand years at most) that was initially suggested for these rocks. Here, we present new detailed magnetostratigraphic data of the Mirassol d'Oeste cap dolostones (Mato Grosso, Brazil) and "bomb-spike" calibrated AMS ^{14}C data of microbial mats from the Lagoa Vermelha (Rio de Janeiro, Brazil). We also compile sedimentary, isotopic and microbiological data from post-Marinoan outcrops and/or recent depositional analogues in order to discuss the deposition rate of Marinoan cap dolostones and to infer an estimation of the deglaciation duration in the snowball Earth aftermath. Taken together, the various data point to a sedimentation duration in the range of a few 10^5 years.

1. Introduction

The Neoproterozoic era is punctuated by several glacial events, among which two at least are regarded as global, in agreement with the so-called *snowball Earth Hypothesis* (Kirschvink, 1992; Hoffman et al., 1998). This was suggested by the presence in most continents of low-latitude glacial deposits (diamictites and tillites) usually overlain by "cap" carbonates (dolostone and limestone) with peculiar sedimentary features and negative carbon isotope signatures (Kennedy, 1996; Kaufman et al., 1997). This uncommon geological succession implies severe and rapid climatic changes from ice-house to hot-house conditions. Duration of glacial intervals is consistently constrained to 3–12 million years by the presence of magnetic reversals in glacial deposits (Sohl et al., 1999), thermal subsidence modeling (Hoffman et al., 1998), as well as resulting iridium anomalies (Bodiselitsch et al., 2005). Estimation of the deglaciation duration, by its turn, is more controversial and can only be constrained by the cap dolostone record, as these rocks were recently demonstrated to have been deposited during the glacioeustatic sea level rise that was induced by land ice melting (Hoffman et al., 2007).

High sedimentation rates for the cap dolostones were initially invoked to interpret their isotopic compositions and sedimentological features, hence a total duration of sedimentation of a few thousand years (Hoffman and Schrag, 2002; Hoffman and Li, 2009). More recently, these estimations were challenged by the record of magnetic reversals in cap carbonates of Brazil suggesting a much slower deposition in the order of 10^5 to 10^6 years (Trindade et al., 2003). Magnetic reversals in Marinoan cap carbonates were further confirmed by results from Oman (Kilner et al., 2005). So far, these magnetic data represent the only way to estimate the sedimentation duration of the cap dolostones and, therefore, the deglaciation duration.

In the present paper we attempt to compile stratigraphic, sedimentary, paleomagnetic, isotopic and microbiological data in order to evaluate the deposition rate and duration of Marinoan cap dolostones and to infer an estimation of the deglaciation duration in the snowball Earth aftermath. New data as well as already published data will be used. We will focus on the Mirassol d´Oeste (MO) cap dolostones (Mato Grosso, Brazil), for which a Pb–Pb age of 627 ± 32 Ma was recently obtained by Babinski et al. (2006). Nevertheless, other well-known cases, such as the Marinoan Keilberg cap dolostones from Namibia (Hoffman et al., 2007), will be also part of the discussion. Interpretation of this Ediacarian geological record will also be enlightened by potential recent analogues, such as the land ice melting following the Last Glacial Maximum and the microbially-mediated dolomite formation in hypersaline lagoons (Lagoa Vermelha, Rio de Janeiro, Brazil).

* Corresponding author. IDL, Faculdade de Ciências da Universidade de Lisboa, EdifícioC8, sala 8.3.22, Campo Grande, 1749-016, Lisboa, Portugal. Tel.: +351 217500811.
E-mail address: font_eric@hotmail.com (E. Font).

0031-0182/$ – see front matter © 2010 Elsevier B.V. All rights reserved.
doi:10.1016/j.palaeo.2010.05.039

2. The stratigraphic and sedimentary record

2.1. Data

In most continents, Marinoan cap dolostones sharply overlie terminal glaciogenic strata (or equivalent hiatus) and represent the transgressive system track (TST) of the post-glacial depositional sequence, i.e. they were deposited during the melting of grounded ice sheets (Hoffman et al., 2007). In Namibia, both isotopic composition and sedimentologic features from the bank and the slope argue for a diachronous sedimentation of the cap dolostones (Keilberg Formation) and their overlying limestones (Maieberg Formation). The transition from dolostones to limestones (Maieberg Formation) is marked by a maximum flooding surface corresponding to the post-glacial high stand sea-level and/or to a chemocline, i.e. to an oxic–anoxic boundary in the water column (Hoffman et al., 2007). The same authors reconstruct the complete $\delta^{13}C$ isotopic record from the different slope and bank sections and obtain a sigmoidal curve over time evidencing a 4.4‰ decline in average as well as a lateral gradient from the inner to the outer bank.

Cap dolostones are characterized by peculiar sedimentary features whose origins are still strongly debated (Kennedy et al., 2001; Hoffman and Schrag, 2002; Allen and Hoffman, 2005; Corsetti and Grotzinger, 2005; Font et al., 2006a; Hoffman et al., 2007). Their transgressive character is supported by the vertical asymmetry of the cap dolostone sedimentary features, low-angle cross stratifications toward the base and giant wave ripples toward the top, indicating water deepening with stratigraphic height. The intermediate sequence is represented by undulated microbialites associated with tube-like structures and fenestral porosity. Tube-like structures are invariably oriented in the paleo-vertical irrespective of the attitude of the host lamination and filled by primary microbial dolomicrite laminated normal to the tube axes (Hoffman and Schrag, 2002; Font et al., 2006a). Their origin is not yet well known but a byproduct of microbial-sediment interaction is a more suitable interpretation (Corsetti and Grotzinger, 2005; Hoffman et al., 2007) than methane seepage (Kennedy et al., 2001; Jiang et al., 2003). Upsection, giant mega-ripples are systematically found just below the transition from dolostones to limestones and the Maximum Flooding Surface. In the Otavi Platform, Namibia, mega-ripple crestlines are parallel and oriented oblique to the bank edge and are interpreted to have formed under perpetual waves with unusually long-wave periods (Allen and Hoffman, 2005).

2.2. Discussion

2.2.1. Interpretation of the sedimentary features

It is hard to evaluate the cap dolostone deposition rate from the previously described sedimentary features. The base (planar to low-angle cross-lamination) and the top (giant megaripples) of MO (MO) and Keilberg Formations result from mechanical deposition, whereas a microbial origin is assumed for the tubestone stromatolite facies. The fact that the tubes are incompletely filled by primary dolomicrite (Corsetti and Grotzinger, 2005) suggests a relative low sediment flux for this facies. However, Grotzinger and Knoll (1999) examined the microbial response to sediment flux and concluded that growth and morphology of stromatolites is controlled by sedimentation rate as well as by other factors such as the specific nature of the mat-building community. Sedimentation cannot have been rapid enough to outpace the microbial response. However, a minimum sediment influx would be required to induce the mat community to propagate upward. Therefore, it is not possible to derive precise information from the domal and tubestone stromatolitic facies. By contrast, giant megaripples aggrading up to 2.5 m of sediment in a single set in Namibia suggest a more rapid sedimentation towards the top of the cap dolostones.

2.2.2. Duration of the sea-level rise

The cap dolostones were deposited during the post-glacial transgression, thus concomitantly with the land ice retreat. Careful observations made by Hoffman et al. (2007) in Namibia suggest that the post-Marinoan sea-level rise was at least 500 m. Therefore, an estimation of the duration of this deglaciation is provided by the maximum duration of the cap dolostone formation. This was first inferred assuming a short duration of a few thousand years by analogy with the recent glacial–interglacial history. However, a more detailed examination of the recent deglaciation considered with the peculiarities of the post-Marinoan case suggests possibly different rates.

The sea-level rise following the recent Last Glacial Maximum (LGM: 21,000 BP) is well constrained at ca. 130 m by far field data in tectonically stable areas, such as the Barbados and Tahiti fossil coral record (Bard et al., 1990, 1996). After the required corrections for both glacio- and hydro-isostasy, the correlative global change in ice volume is 52×10^6 km^3 (Lambeck et al., 2000) and most of this volume is explained by the disappearance of the Laurentide ice sheet. However, sea-level rise did not occur in a linear way after the LGM. Depending on local conditions, each ice sheet had its own evolution (Bentley, 1999). Thus, modelling experiments point that the Antarctic ice sheet reached its maximum volume at 10,000 BP well after the LGM; ice retreat was complete at 5000 BP in Greenland, whereas it still continues today in West Antarctica and will do so for another 1000 years in the future (Huybrechts, 2002). However, both Greenland and Antarctica are high-latitude ice sheets and, hence, they were not the main contributors to the post LGM sea-level rise. The broadly sigmoidal shape of the sea level curve witnesses that ca. 80% of the sea level rise, i.e. 100 m rise, occurred between 15,000 and 7000 BP (Peltier and Fairbanks, 2006). This 8000 years time lag corresponds to the retreat of most of the lower-latitude Laurentide and Fennoscandian ice sheets. In addition, three periods of rapid sea-level rise have been identified, namely at ca 19,000 BP (Clark and Mix, 2000), and especially at 14,000 BP and 11,000 BP (Bard et al., 1990, 1996). These so-called melt water pulses, that were responsible for sea level rise up to 3 m per century (Bard et al., 1990), disturbed the oceanographic and climatic regimes for a few hundreds of years, hence a noticeable temporary cooling effect. Calculation of the duration of the post-Marinoan 500 m sea-level rise by comparison with the recent post-glacial events cannot be straightforward. One reason is that the melting rates of low-latitude ice sheets that would have formed during the Neoproterozoic ice ages is likely to be faster than the melting of higher-latitude ice sheets. Indeed, palaeogeographic reconstructions at ca. 635 Ma show that most continents were distributed in the zonal interval from 40°N to 60°S (Trindade and Macouin, 2007; Hoffman and Li, 2009). However, although we have paleomagnetic evidence that ice extended as low as the intertropical zone, we know neither the zonal distribution of the Neoproterozoic ice-sheets nor their extent and thickness. Assuming that post-glacial sea level rise occurred at the same average speed than most of the post-LGM rise, i.e. 100 m rise in 8000 years, the calculated duration for 500 m rise is about 40,000 years. However, deglaciation is not necessarily linear (Charbit et al., 2002; Bamber et al., 2007). Workers that suggested a shorter duration for the post-Marinoan deglaciation argued that air temperatures should have been much higher than today due to the very high atmospheric CO_2 and because of the positive feedback due to melting ice and consequent albedo decrease. Nevertheless, the temperature gradient in the atmosphere above the ice sheets remains equivocal and a high temperature at the surface of the ocean (e.g. 30 °C after Higgins and Schrag, 2003) is unlikely at the beginning of the deglaciation, especially because the surface water may have been cold melt water for some time. A peculiarity of the snowball and immediate post-snowball climate arises from the possible occurrence of sea glaciers, that would have flown equatorwards from mid-latitude and polar thick sea-ice areas (Goodman and Pierrehumbert, 2002; Warren et al., 2002; Pollard and Kasting, 2005).

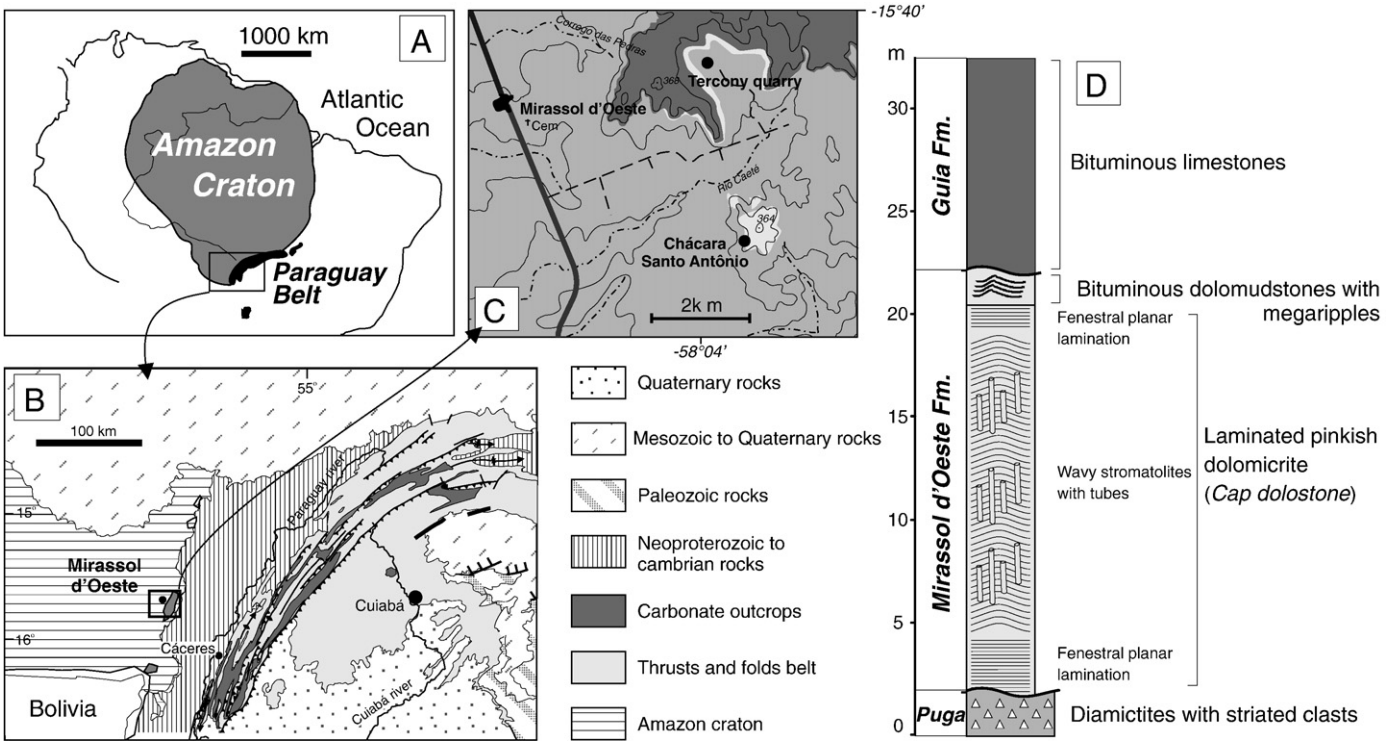

Fig. 1. Location of Amazon craton (A) and Paraguay belt (B) (modified from Nogueira et al., 2003). Geological map of the studied sector (C) with localization of Terconi section (TR) and regional stratigraphic sequence (D).

Goodman and Pierrehumbert (2002) calculated that melting of the front of sea glaciers at 20–25° latitude results in a very efficient cooling effect in the tropics, because ice melting requires latent heat and delivers cold fresh waters that will not mix easily in the ocean. Taken together, these considerations suggest that post-Marinoan deglaciation may have persisted for a minimum of 40,000 years and possibly longer depending on the existence of sea glaciers. So far, no detailed numerical modelling of the melting of the snowball Earth has been attempted. Hyde et al. (2000) present various simulations yielding temperature, sea ice and land ice volume with variable CO_2 levels using either an energy-balance model (EBM) or an EBM coupled to an ice sheet model. Both types of simulations give different results and indeed, with the ice sheet model, no deglaciation occurs during warm summer orbital configurations because of ice elevation and the long time constant associated with the melting of thick ice. They also state that, with atmospheric CO_2 at 1000 PAL (present atmospheric level), the deglaciation is very rapid, with a duration of only 2000 years. However, they do not show the corresponding modelling and therefore it is difficult to discuss the result obtained at such a high, maybe unrealistic, pCO_2. Climate modeling including both land ice and sea ice retreat in post-snowball Earth conditions is obviously required to elucidate the point.

3. The paleomagnetic record

3.1. Data

Paleomagnetic data of Marinoan and Sturtian cap dolostones indicate the presence of magnetic reversals. A dual polarity magnetic component for Sturtian dolostones was first identified by Li (2000) in the Walsh Tillite in Australia (only one reversal). Strong evidence of several stratabound reversals in Marinoan cap dolostones of Brazil was first documented by Trindade et al. (2003) and confirmed by further studies in Oman (Kilner et al., 2005) and Australia (Raub and Evans, 2005). In Oman, however, only one reversal is identified along the cap dolostone section and paleomagnetic data from Australia have not been published in detail (Kilner et al., 2005; Raub and Evans, 2005) making the MO (MO) cap dolostones from Brazil the most reliable for detailed magnetostratigraphic analysis.

The first paleomagnetic results of the MO cap dolostones, dated at 627 ± 32 Ma (Pb–Pb, Babinski et al., 2006), provided a 22° paleolatitude for the Amazon craton and passed the reversal test of McFadden and McElhinny (1990) (Trindade et al., 2003). Detrital hematite as the main magnetic carrier, in absence of secondary iron oxides and superparamagnetic particles, suggests that the characteristic magnetic signal is primary (Font et al., 2005). Furthermore, upper limestones had given a secondary magnetization (negative fold test) dated at around 520 Ma giving a minimum age for the dolostone remanence (Font et al., 2006b). Here, 68 paleomagnetic sites yielded 229 samples, with a sampling interval of approximately 20 cm. (Fig. 1.C). The mean paleomagnetic direction obtained at each site (Table 1) matches the directions obtained in our earlier work (Trindade et al., 2003). After transforming the TR normal directions into reverse antipodal directions, a reverse mean component was calculated ($D = 184.5°$; $I = -37.2°$. $N = 134$; $\alpha_{95} = 2.5$). The corresponding virtual geomagnetic pole (VGP) is localized at Long = 260.9°; Lat = −83.6° (Dp = 1.7; Dm = 2.9) with a

Table 1
Sample- and site-based mean paleomagnetic directions of the Terconi Quarry (TR) and corresponding Virtual Geomagnetic Poles.

	Mean directions						VGP			
	N	*D* (°)	*I* (°)	α_{95} (°)	*k*	*R*	Long. (°)	Lat. (°)	Dp	Dm
Sample-based mean										
TR normal	36	2.3	−33.9	2.9	67	35	261.8	−86.6	1.9	3.3
TR reverse	79	185.7	41.7	3.7	19	75	269.2	−80.4	2.8	4.5
Site-based mean										
TR normal	20	2	−34.3	4.1	64	19	268.3	−86.6	2.7	4.7
TR reverse	36	182.5	40.3	4.6	27	34	283.7	−82.6	3.4	5.6

corresponding paleolatitude of 20.8°. At least five reversals (instead of four in the previous study) are identified in the sedimentary column of the Terconi quarry (TR) section (Fig. 2). At the top of the sequence, a reversal was recorded in only one paleomagnetic site (site TR5.P) and thus was not considered as an interval of polarity.

In order to check for the variation of the paleomagnetic field at a finer scale, we have cut samples from the contact with diamictites into adjacent cubes of 2×2 cm, from a grid of 5 vertical columns (named A to E) and 7 horizontal lines (numbered 1 to 7) which are roughly parallel to the stratification plane. This method does not allow accurate paleomagnetic mean calculations, because of the systematic error induced by the block orientation, but allows us to study more precisely the secular variation record of the detrital remanence. Magnetic variations show a coherent pattern from the base to the top, with declination values decreasing continuously towards the top (Table 2, Fig. 3). Along 14 cm of cap dolostone, the maximum difference between the base and the top reach 7° (column B) for the magnetic declination and cannot be illustrated on the stereographic projection.

3.2. Discussion

3.2.1. Reversals

The geomagnetic pole position of the Earth's magnetic field is subject to variations of different time-scale. Variations with periods of a year to hundred thousands of years are generally referred to as *geomagnetic secular variation*. The origin of geomagnetic secular variations can be subdivided into two contributions with overlapping periodicities: non-dipole changes dominating the shorter periods (less than 3000 years) and changes of the dipolar field with longer periods. Over historic time, there has been a tendency for some features of the non-dipole field to undergo a longitudinal shift toward the west, the so-called *westward drift* (Bullard et al., 1950). On longer time scales, the dipolar geomagnetic field produces a 180° change in surface geomagnetic field direction at all points, called a *geomagnetic field reversal* (Mercanton, 1926; Matuyama, 1929; Cox et al., 1964).

Long-term variations of the geomagnetic field polarity are not entirely a periodical phenomenon and the time scale of polarity reversion varies greatly throughout the history of the Earth (e.g. Merrill et al., 1996). A Geomagnetic Polarity Time Scale (GPTS) is well established for the past 160 Myr from the marine magnetic anomalies record, but the frequency of geomagnetic reversals at the end of the Neoproterozoic is totally unknown. Kirschvink (1979) found several magnetozones in the Late Precambrian to Early Cambrian sediments of the Amadeus Basin, Central Australia, for which a primary character of the magnetization was documented by fold and unconformity tests. Sohl et al. (1999) provided distinct polarity magnetozones for both the Yaltipena and Elatina Formations (glaciomarine and early post-glacial) and suggested that the polarity stratigraphy of the Elatina Formation could encompass as much as several millions of years, depending on the rate of reversals in Neoproterozoic time. A long zone of reverse polarity is identified just below the Precambrian–Cambrian boundary, followed by a zone of mixed polarities during the Cambrian (Gallet et al., 2003). A superchron of ~25 Myr was suggested by Gallet

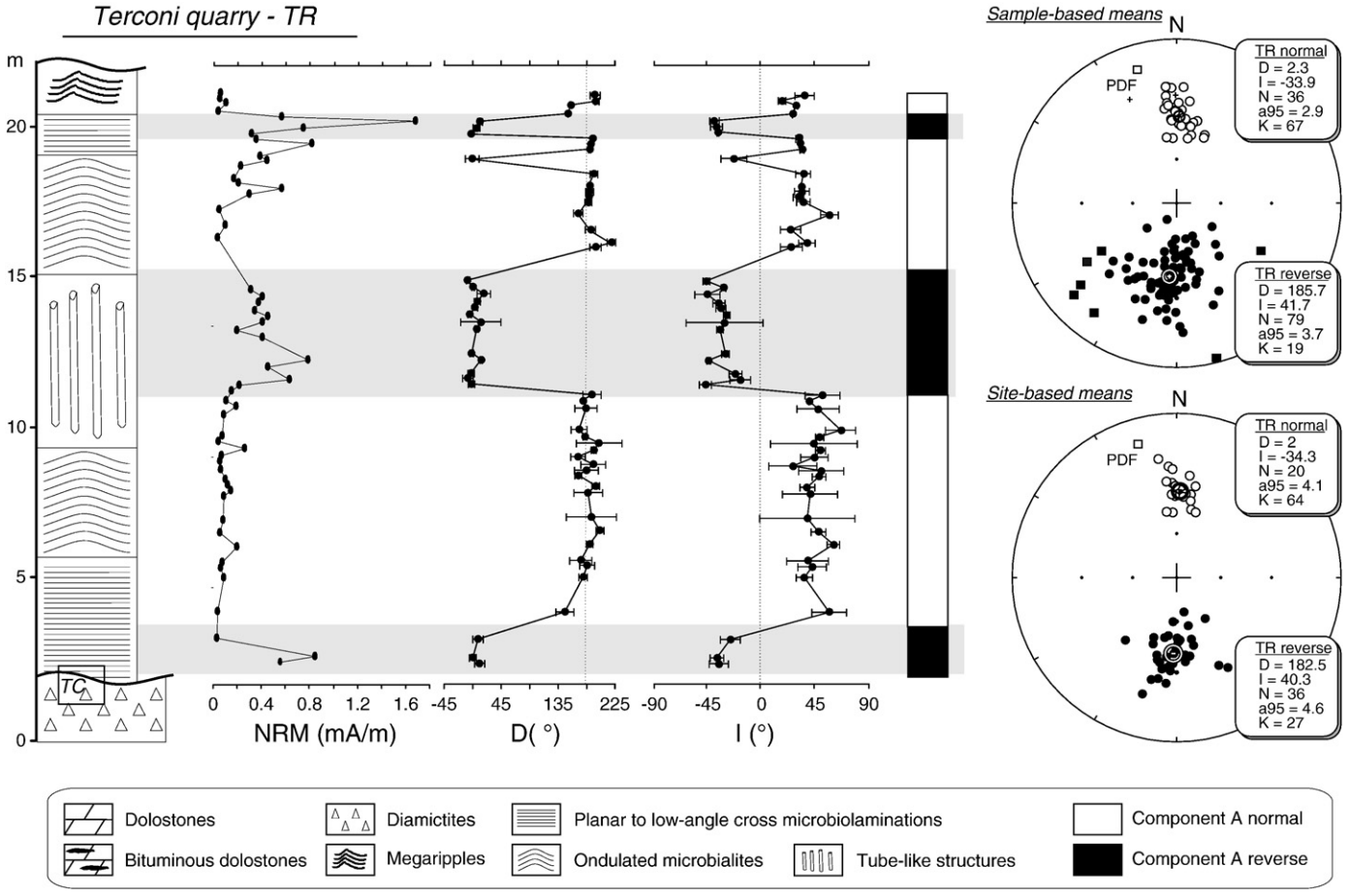

Fig. 2. (*On the left*) Magnetostratigraphic data of the Terconi section giving declination (D) and inclination (I) obtained on each paleomagnetic site. A polarity scale is provided. (*On the right*) Stereographic projections of sample-based and site-based mean from TR section. The Present-Day Field (PDF) is also indicated. Square symbols from sample-based mean directions correspond to data excluded for the mean component calculation.

Table 2
Paleomagnetic directions ($D°$, $I°$, α_{95}) of small samples (cubes of 2×2 cm) collected from the basal contact with diamictites. The grid is composed of four columns (A,B,C and D) and seven horizons which are oriented parallel to the stratification plane. A mean for each horizon is also given and represented in the stereograph of Fig. 3.

Sample	*d* (cm)	*D* (°)	*I* (°)	α_{95}
A1	0	3.1	−32.1	6.6
A2	2	4.7	−28.2	3.9
A3	4	7.9	−34.3	4.2
A4	6	5.4	−26.4	5.6
A5	8	5.8	−31.7	6.1
A6	10	4.6	−28	4.5
A7	12	3.6	−35.5	9.5
B1	0	9	−32.3	5.9
B2	2	6.5	−32.2	3.4
B3	4	8.5	−34.2	4.5
B4	6	5.5	−31.4	5.3
B5	8	5.5	−32	8.8
B6	10	4.8	−30.6	7.4
B7	12	2.3	−34.1	6.7
C1	0	9.9	−40.2	4.3
C2	2	5.7	−31.4	2.9
C3	4	9.6	−27	3.2
C4	6	4.8	−36.2	4.5
C5	8	4.3	−35.6	3.8
C6	10	5.3	−28	7
C7	12	4.8	−34.1	6.4
D1	0	4.9	−38.7	1.5
D2	2	4.7	−36.7	3.9
D3	4	5.5	−28	5.7
D4	6	2.9	−33.2	6
D5	8	3.2	−31.5	9.8
D6	10	2.7	−24.5	7.3
D7	12	2.6	−31.8	8.2
Mean	N	D (°)	I (°)	α 95
TC1	4	6.7	−35.9	5.7
TC2	4	5.4	−32.1	4.1
TC3	4	7.9	−30.9	4.8
TC4	4	4.7	−31.8	4.8
TC5	4	4.7	−32.7	2.5
TC6	4	4.3	−27.8	3.1
TC7	4	3.3	−33.9	2

et al. (2003) from the Lower Ordovician to the Middle Ordovician. The upper part of the Middle Cambrian seems to be characterized by high frequency of magnetic reversals.

The new paleomagnetic results presented here indicate at least five reversals within 20 m of the MO dolostones demonstrating a high-frequency geomagnetic field reversal at around 635 Ma. It also provides a powerful chronologic tool to estimate the minimum deposition time of cap dolostones and consequently the time of ice-melting after a snowball Earth event. However, the paucity of magnetostratigraphic data during Precambrian time makes it difficult to estimate the reversal frequency in Marinoan cap dolostones. As a first approximation, the magnetic record indicates that complete reversals of polarity may average 2–3 per million years with a maximum of 4–6 reversals per million years in the Miocene, Jurassic and Cambrian (Gallet and Courtillot, 1995; Merrill et al., 1996; Pavlov and Gallet, 2001; Gallet et al., 2003). In comparison to middle Cambrian data (Gallet et al., 2003), the number of Neoproterozoic reversals forces the reconsideration of the cap dolostone deposition time span of 10^3–10^4 years proposed by Hoffman and Schrag (2002). Assuming that Marinoan cap dolostones were deposited in 10,000 years should correspond to a reversal frequency of 500 per million years. This is not compatible with dynamo models (Gubbins, 1999; Wicht and Olson, 2004). Rather, a minimum interval of 10^5–10^6 years is suggested for the MO cap dolostones deposition. Hence, taking a conservative value of 6 to 8 reversals per Ma as the maximum value, the presence of five reversals in the 20 m of MO dolostones would give a minimum and maximum sedimentation rate of 0.0024 cm/yr and 0.0032 cm/yr respectively, hence a time deposition period of 600,000 to 800,000 years.

3.2.2. Lack of secular variation record

The timing of geomagnetic secular variations is quite difficult to evaluate, particularly in older geological times, but roughly corresponds to periods of a year to thousands of years. The secular variation of the magnetic field was first checked by the systematic measurement of the remanent magnetization in lake sediments by Mackereth (1971). The variation curves established from volcanic lakes of the northern hemisphere (e.g. Smith and Creer, 1986; Thouveny et al., 1990) and of the equatorial region (Thouveny and Williamson, 1988) are quite similar, whereas curves from the southern hemisphere display a different periodicity (Barton and McElhinny, 1981). In any case, variation amplitudes are up to 80° in declination and 30° in inclination with a period of a few kyrs. A record of secular variation in sediments requires continuous sedimentation with a rate of at least 10 cm/kyr. Conversely, the lack of secular variation is evidence of a slow sedimentation rate, with each sample yielding averaged declination and inclination. This is the case in Mirassol d'Oeste, pointing to a sedimentation rate likely lower than 10 cm/kyr.

4. The continental weathering record

Because the post-glacial transition is associated to high atmospheric CO_2 (~660 PAL equivalent to 0.2 bar to melt ice sheet; Pierrehumbert, 2004), high weathering rates were inferred by Hoffman et al. (1998) and Higgins and Schrag (2003), consistent with the high delivery of Ca and continental alkalinity required to precipitate the cap dolostones (Higgins and Schrag, 2003). The continental weathering record is therefore worth of consideration as a possible way to set limits on the duration of cap dolostone formation.

4.1. Data

4.1.1. Elemental and isotopic data

Weathering rates at the snowball Earth aftermath are a crucial parameter that controls the thickness, i.e. the deposition rate, of cap dolostone by delivering the required Ca, Mg and alkalinity to the ocean. Reduced weathering rates in the snowball Earth aftermath is a plausible explanation for the poor detrital supply noted in cap dolostone despite their continental setting (Font et al., 2005). The increase of chemical and mineralogical indices of alteration (CIA and MIA) from glacial (Sturtian) to post-glacial sequences in Oman is gradual (Rieu et al., 2007a,b). The maximum values corresponding to the maximum weathering rates are located in the Arkahawl Formation, 150 m above the cap carbonates that overlie the glaciogenic Ayn Formation (Rieu et al., 2007a). Although these elemental and geochemical data were obtained from a post-Sturtian succession, they appear in good agreement with Sr and Ca isotope data from younger successions elsewhere, which suggest that the maximum silicate weathering rate is reached only after cap dolostone deposition (Alvarenga et al., 2007; Nédélec et al., 2007; Nogueira et al., 2007), i.e. after the melting and transgressive phase, as discussed below. Similar results were obtained from Marinoan sections of Oman, namely Hadash (glacial) and Mashira Bay (cap carbonates) Formations but no data are provided for the cap dolostone interval (Rieu et al., 2007b).

Strontium isotopic compositions can be used as a proxy to estimate the silicate weathering rates at the aftermath of the snowball Earth. The recent compilation of Halverson et al. (2007) provides a long-term evolution of the $^{87}Sr/^{86}Sr$ record in marine carbonates throughout the Neoproterozoic. Although the values abruptly rise at the end of the Marinoan glaciation, precise $^{87}Sr/^{86}Sr$ data are few and the cap dolostone section is not always well documented due to low

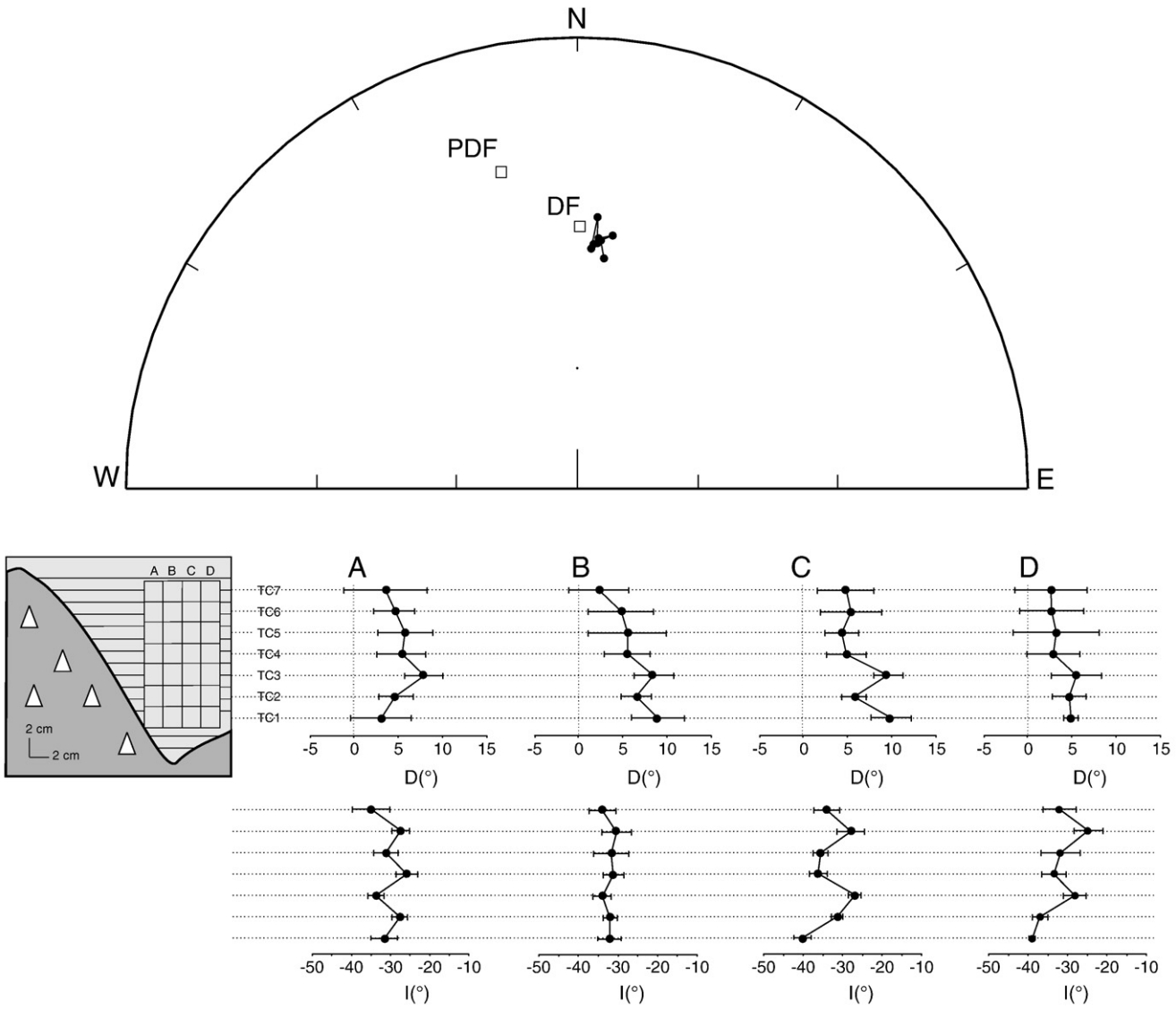

Fig. 3. Detailed paleomagnetic directions of TC sites obtained from cubic samples collected in a grid of 14 × 8 cm (one mean-site direction for each 2 cm) from a bloc localized just above the contact with Puga diamictites. Maximum Angular Deviation (MAD) for each sample is indicated.

Sr concentration in dolomite (Kaufman et al., 1997; Nogueira et al., 2003; Alvarenga et al., 2007; Nédélec et al., 2007; Nogueira et al., 2007). However, existing data suggest that the peak of silicate weathering, most likely correlated to the warmest and most humid climatic conditions, is decoupled from the nadir of carbon isotope signatures and occurs in rocks younger than the proper cap dolostones.

Recently, B and Ca isotopic data of Marinoan (post-Ghaub) Namibian cap carbonates provided important clues about pH ocean chemistry and weathering rates of the postglacial greenhouse transition (Kasemann et al., 2005). A negative $\delta^{11}B$ excursion is registered in the Keilberg cap dolostones and interpreted as a temporary decrease in seawater pH in response to rapid CO_2 transfer from the atmosphere to the surface ocean. The return to higher values occurs at the top of the dolostones. The $\delta^{44}Ca$ isotope pattern displays a different evolution from $\delta^{11}B$, with decreasing $\delta^{44}Ca$ values from the top of the dolostones of the Keilberg Formation until the middle part of the limestone of the Maieberg Formation (~100 m above the diamictites), after that $\delta^{44}Ca$ values increase until the top of the Maieberg Formation. The $\delta^{44}Ca$ is an inverse proxy of the ratio of calcium fluxes into and out of seawater (Kasemann et al., 2005). Therefore, the highest weathering fluxes (Ca input) with respect to carbonate sedimentation rates (Ca removal) seem to have been delayed after the cap dolostone deposition.

4.1.2. Numerical modelling data

Numerical simulations of Higgins and Schrag (2003) are based on assumed high precipitation rates, high surface temperatures, low meteoric and soil water pH and on the extensive occurrence of unweathered rock powder (loess), hence high silicate weathering rates. These authors used unconstrained values of 5, 10 and 17 GtC/yr for the corresponding effects of intense silicate weathering. In this hypothesis, strong silicate and carbonate weathering would have rapidly supplied the amount of dissolved Mg and Ca required for precipitation of the cap dolostone (Hoffman et al., 1998) and also would have rapidly drawn down the atmospheric CO_2, i.e. after only some 10^3 years. Recently, Le Hir et al. (2009) explored more rigorously the post-snowball climate using an atmospheric general circulation model (FOAM 1.5) with the 635 Ma palaeogeography, and a kinetic weathering model (WITCH). They show that, even under very high pCO_2, (e.g. 400 PAL), the run-off is only 22% higher than the calculated present day value. In the same conditions, they also show that weathering rates are strongly dependent of the mineral reactive

surface. However, the persistence of a hydrological cycle during the glacial epoch would not allow the formation of a thick soil profile (Donnadieu et al., 2003). A 1.25 m-thick soil profile is used in the simulations. Applying the reactive surface value measured on loess derived from the LGM, Le Hir et al. (2009) obtain a 10-fold increase of CO_2 consumption by silicate weathering with respect to the modern value calculated by Gaillardet et al. (1999). However, at lower pCO_2 (10 PAL), CO_2 consumption rate is about 10-fold less than present day values, especially because of the lack of biotic effects in the soils. As a whole, the models yield cation and CO_2 consumption fluxes for 8 FOAM climate scenarios from 400 PAL CO_2 to 10 PAL. Modelling the evolution of atmospheric CO_2 is obtained using these results and the COMBINE model that calculates the alkalinity and carbon budget of ocean and atmosphere, as well as the carbonate speciation in the ocean (Goddéris and Joachimski, 2004). Le Hir et al. (2009) provide four resulting curves of atmospheric CO_2 versus time after melting, depending on various cases of reactive mineral surface and soil thickness. Whatever the case and starting from 400 PAL, CO_2 is still above 100 PAL after 10^5 yrs. With a highly reactive surface and 1.25 m-thick soil, the time to restore atmospheric pCO_2 to its pre-glacial values due to the silicate alteration sink is likely on the order of a few million years. With a thicker soil (6 m, a more favourable, but likely less realistic value), the time required is still 2 million years.

4.2. Discussion

Both elemental and Sr and Ca isotope records do not provide direct estimations of the duration of the cap dolostone formation, but they set an upper limit for this duration because the maximum silicate weathering seems to have occurred well after the end of the cap dolostone deposition. As silicate weathering is first controlled by climatic conditions, these data also suggest that the immediate post-snowball climate was not as warm and humid as inferred by Higgins and Schrag (2003). This is confirmed by the climate and weathering modelling of Le Hir et al. (2009), which indicate that it took at least 2 million years to consume the excess of atmopsheric CO_2 by silicate weathering, hence setting also some limits to the rate of cation delivery to the ocean. This calculated time lag sets a maximum duration for the cap dolostone deposition because these rocks were deposited clearly before the silicate weathering maximum as evidenced by elemental and isotopic sediment geochemistry.

Regarding the duration of cap dolostone deposition, it may be more appropriate to consider the carbonate weathering rate rather than the silicate weathering rate. The increased Ca supply is first provided by rapid carbonate weathering at the front of the retreating glaciers, a much more active process than silicate weathering during the ice melting phase (Anderson et al., 2000). Indeed, at very low temperatures such as in ice melt waters (1 °C), the solubility of carbonates is increased, whereas silicate weathering is inhibited. In addition, it is worth to notice that the $\delta^{44}Ca_{cc}$ values in the cap dolostones are not lower than some pre-snowball values and are also in the range of recent Ca isotope data (Kasemann et al., 2005). This observation does not contradict the suggestion of higher carbonate weathering rates after deglaciation, as $\delta^{44}Ca_{cc}$ values do not directly reflect the Ca input (due to continental weathering), but rather constrain the balance between the Ca input and the Ca output (by carbonate precipitation). Hence, the post-snowball record is consistent with both a high Ca input (due to high carbonate weathering rate) and a high Ca output (corresponding to the coeval worldwide cap dolostone sedimentation).

Finally, it is worth to model calcium and alkalinity delivery by carbonate dissolution during the melting phase. Adding exposed carbonate platforms along the coast line and inland carbonate outcrops (with a present-day extent) in their weathering model and using a simple eustatic model and an assigned global climate (1 °C, run off of 20 cm/yr and 1000 PAL CO_2 at the very beginning of deglaciation), Le Hir et al. (2009) show that, considering a deglaciation timescale of 10 kyr, the resulting dissolved element discharge from carbonate (and minor silicate) weathering into the ocean would only account for a cap dolostone deposition of 50 cm in thickness. Hence a time of 400,000 yrs would be required for deposition of 20 m of dolostone. Taking into account only a 5 m-thick value as the characteristic average of cap dolostones would still require at least 10^5 years, that is regarded as the minimum duration for cap dolostone deposition.

5. The microbial record

After two centuries of research about the Dolomite Problem (Land, 1998; Burns et al., 2000; Warren, 2000), the precipitation of primary dolomite is still debated. In the aftermath of a snowball Earth event, the predominance of dolomite received different explanations. Hoffman et al. (2007) consider that seawater was characterized by a low sulphate concentration favoring abiotic dolomite precipitation, as sulphate ions are a well-known inhibitor of dolomite (Baker and Kastner, 1981), because of the links established between Mg and sulphate. In addition, Higgins and Schrag (2003) explained the cap dolostones negative carbon isotope signatures by the disappearance of nearly all living beings in the snowball Earth harsh conditions. This last hypothesis is no more tenable at the light of recent discoveries as shown below.

5.1. Data

Recently, we proposed that the cap dolostones from Brazil and Ghana had precipitated in suboxic conditions influenced by sulphate-reducing bacteria activity (Font et al., 2006a; Nédélec et al., 2007) pointing to a microbially-mediated model for dolomite precipitation, in the same way as the recent analogues from the Lagoa Vermelha coastal lagoon (Brazil) studied by Vasconcelos and McKenzie (1997) and van Lith et al. (2003a,b). Indeed, the studied cap dolostones of Brazil (MO) and Ghana (Bwipe) locally display sedimentary features resembling fossil microbial mats (Font et al., 2006a; Nédélec et al., 2007). Their laminations are evocative of lithified stromatolites, in as much as stromatolites build ups were indeed recognized in some cap dolostones. Carbon isotopic compositions of microbially-mediated dolomites in Lagoa Vermelha are around −3‰ in the deeper part of the present microbial mat (Vasconcelos et al., 2006), values close to those of common Neoproterozoic cap carbonates and also consistent with some contribution of organic carbon-derived bicarbonate ions to the precipitation of these rocks. Ader et al. (2009) show that shelf-to-basin lateral variations of carbonate and organic matter isotopic C signatures in the Ediacaran Yangtze platform are compatible with a stratified water column. In most cases, an oxic surface layer in equilibrium with the atmosphere lies above an euxinic layer with lower (negative) $\delta^{13}C_{DIC}$ (dissolved inorganic carbon) due to organic matter oxidation by ongoing sulphate reduction. Locally, a third deeper layer may form in the inner shelf with a higher (positive) $\delta^{13}C_{DIC}$ due to methanogenesis. Although their study encompasses all post-marinoan carbonates and not only the basal cap dolostones, it is another piece of evidence that alkalinity derived from incomplete degradation of organic matter contributed to post-glacial carbonate precipitation and that the global C isotope signatures of carbonates may have been influenced by local effects.

We now know that many resistant forms of life could have survived during a snowball Earth event and bloomed in its aftermath (Corsetti et al., 2003; Corsetti and Grotzinger, 2005; Olcott et al., 2005; Corsetti et al., 2006; Elie et al., 2007). In modern-day polar regions, microbial mats can survive in association with many protist and metazoan species under thick landfast sea ice. Cyanobacteria communities, in particular, show an extreme tolerance for low temperatures (Vincent and Howard-Williams, 2000). Besides, Anderson et al. (2000) pointed

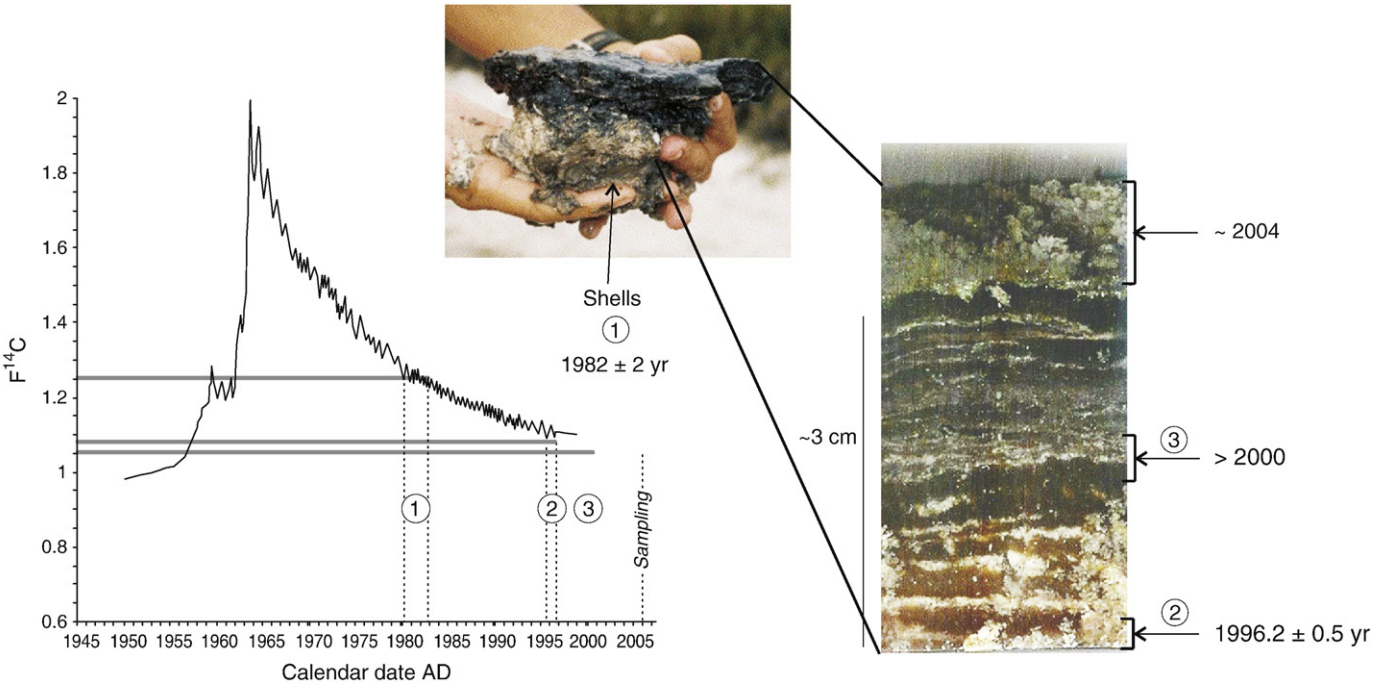

Fig. 4. Photographs of microbial mats from the Lagoa Vermelha, Brazil and their corresponding AMS ^{14}C dating calibrated with data of Marshall et al. (2007).

out that sulphide oxidation is particularly important at the weathering front of modern retreating glaciers. In post-Marinoan times, sulphate is also likely to have been delivered by proglacial streams, hence sulphate was available in the shallow waters along the coast where dolomite precipitated. Although some workers postulate a lesser amount of oxygen in the atmosphere at the end of Precambrian times with respect to the present-day composition, it is worth to notice that marine bacterial sulphate reduction has been evidenced on the basis of S isotope fractionation since the end of Archaean times (Grassineau et al., 2002), hence the surperficial post-Marinoan seawaters are likely to have contained enough sulphate to fuel bacterial sulphate reduction in the sediment. In addition, fossil hydrocarbons sampled at the top of the Mirassol d'Oeste cap dolostone contain biomarkers typical of cyanobacteria, sulphate-reduding bacteria, sulphate-oxidizing bacteria and red algae (Elie et al., 2007).

Assuming a microbially-mediated model for cap dolostones, or at least the peritidal ones, the modern case of primary dolomite precipitation in Lagoa Vermelha (Brazil) is worth considering in detail. Fig. 4 shows photographs of the microbial mat, collected in October 2004 in the Lagoa Vermelha, together with the underlying shell-rich detrital sediment. The microbial mat consists of alternating millimetric-scale dark (organic-rich) and inframillimetric-scale bright (carbonate) layers. The mat surface is covered by a less dense expanded exopolymer layer. Vasconcelos et al. (2006) report that the uppermost layers of the mat are the site of oxygenic photosynthesis leading to calcite precipitation, whereas the underlying anoxic layers are the site of sulphate reduction leading to the precipitation of Mg-carbonates. In an attempt to estimate the mat growth rate and the coeval carbonate sedimentation rate in the Lagoa Vermelha, we have dated three different layers by the "bomb-spike" calibrated AMS ^{14}C technique (Table 3). We considered carbonates globally, without trying to differentiate Ca- and Mg-carbonates. The method is based on the rapid post-1950 increase in atmospheric ^{14}C produced by the above-ground testing of nuclear weapons and has proven its efficiency in dating contemporaneous organic sediment (Goodsite et al., 2001; Turetsky et al., 2004; Marshall et al., 2007). Ages of shell-rich underlying sediments, lower and intermediate layers of microbial mat (organic-rich/carbonate doublets) are reported on the "bomb-spike" calibrated ^{14}C curve of Marshall et al. (2007) (Fig. 4). Radiocarbon ages, calculated following Mook and Van der Plicht (1999), are expressed in pMC (percent modern carbon) and normalized to a δ^{13}C of −25‰ (Table 3). Errors are related to the uncertainty of the radiometric measurement (inferior to the thickness of the line crossing the coordinate axis) and to oscillations of the proper "bomb-spike" calibrated ^{14}C curve. As the Lagoa Vermelha is located in the South Hemisphere and because the "bomb-spike" calibrated ^{14}C curve illustrated in Fig. 4 is calculated for the North Hemisphere, data should be shifted by a time of 6 months. However, this correction is unnecessary because it is already included in the error range of the AMS ^{14}C method used here. On the other hand, datations are not punctual and correspond to a certain thickness of sediment (ca. 2 mm) including both organic-rich and carbonate-rich layers corresponding to one to two doublets.

Considering the normal stratigraphic position of the sampled layers, data are located on the right limb of the "bomb-spike" calibrated ^{14}C curve. Shells from the underlying detrital sediment give an age of 1981.5 ± 1.4 years while the lower part of the microbial mat is dated at 1996.2 ± 0.5 years. Knowing that the upper layer corresponds to the sampling year, i.e. 2004, the growth of the whole microbial mat spans about 10 years. This is consistent with the recognition of at least 10 paired layers in the mat, assuming that the alternation of organic-rich and carbonate-rich layers corresponds to a seasonal cycle typical of a two-season tropical climate (wet summer

Table 3
Radiocarbon ages of microbial mats from Lagoa Vermelha, Brazil, calculated following Mook and Van der Plicht (1999). Mass of carbon (in milligrams) and values of δ^{13}C are indicated. Ages are expressed in pMC (percent modern carbon) and normalized to a δ^{13}C of −25‰.

Sample	Nature	mg C	$d^{13}C$	pMC
Intermediate horizons	Organic matter	0.82	−11.90	105.85 ± 0.29
Lower horizons	Organic matter	0.60	−20.50	108.13 ± 0.29
Shells	Shells	1.70	−5.30	125.42 ± 0.29

and dry winter). Therefore, the mat layering witnesses its annual growth. The mat being ca. 3.5 cm thick (when including the uppermost layer rich in extraxcellular polymers, Fig. 4), the corresponding growth rate would be around 0.3 cm/yr.

5.2. Discussion

The above calculated growth rate of 0.3 cm/yr refers to the most recent Lagoa Vermelha mat. Oven drying of a vertical section of the mat accounts for 30 to 50% weight loss and only 15 weight % of the dried mat are made of carbonates. Hence, the carbonate production in the superficial Lagoa Vermelha sediment is no more than 0.01 cm/yr. This is the minimum carbonate production rate, because it is regardless of subsequent lithification during burial and compaction. Compaction in carbonate is hard to evaluate because it depends on several factors such as depositional texture, early diagenesis, dissolution and reprecipitation, for example, and would be less when lithification and cementation happen early as it is the case for lithified stromatolites (Reid et al., 2000). Subsequent lithification as well as carbonate dissolution leading to the formation of fenestrae may also occur in the sediment. Therefore, assuming that the entire mat would be lithified after sedimentation and compaction, we have a maximum value of 0.2 cm/yr for the formation rate of microbial carbonate. This is the precise range of thickness for the laminations in recent lithified stromatolites (Reid et al., 2000), as well as in the Bwipe cap dolostones (Nédélec et al., 2007). However, the actual growth rate of microbial carbonate is likely lesser, because not all years may be favourable for lithification. Reid et al. (2000) state that lithification of cyanobacterial mats only occurs during quiescent periods with no sedimentation. This is to be compared with another possible recent analogue, namely a lithified carbonate layer formed during the eustatic rise following the LGM in the Red Sea (Brachert, 1999). This aragonitic layer with macroscopic stromatolite fabrics and microscopic laminae likely formed in the 23,000 to 13,000 BP interval, in a situation of restricted marine circulation, low rate of precipitation and high temperature. Brachert (1999) calculates a growth rate of 0.005 to 0.01 cm/yr for this Pleistocene carbonate layer.

Taking into account the previous data from modern and recent microbial carbonate, i.e. a growth rate in between 0.005 and 0.2 cm/yr, gives an interval of 10,000 to 400,000 yrs for the deposition of 20 m of dolostone, assuming that the whole of cap dolostone deposit was formed in this way, with no interruption of sedimentation.

6. Conclusion

Even if an accurate calculation is beyond the scope of our study, the compilation presented here gives us some clues to check for the timescale duration of cap dolostone deposition. All estimations are gathered in Fig. 5. Our new paleomagnetic data matches our previous results (Trindade et al., 2003) and now better identify the presence of at least five reversals in 20 m of cap dolostone. In comparison to middle Cambrian times, pulsed by high reversal frequencies, a minimum interval of 10^5–10^6 years is suggested for the deposition of these dolostones. Furthermore, assuming that post-Marinoan cap dolostones precipitated as microbially-induced rocks by analogy with carbonate precipitation observed in modern microbial mats from the Lagoa Vermelha, Brazil, it is possible to derive dolomite precipitation rates. AMS^{14}C dating confirms that laminations correspond to annual growth. The calculated precipitation rates for microbially-induced dolomite yield a duration of 10,000 to 400,000 years, assuming no interruption of the sedimentation. Considerations relative to the modeled carbonate weathering rate point to a minimum of 400,000 years to dissolve enough carbonate to yield calcium and continentally-derived alkalinity in sufficient amounts to precipitate the cap dolostones. A much longer duration, at least 2 Ma or even more, is required to reach the conditions of maximum silicate weathering, as can be observed from elemental and isotopic data. Taken together, all these approaches support the possibility that cap dolostone deposition lasted for a few tens to a few hundreds of thousands of years (10^4–10^5 yrs), hence the ice retreat was in the same range. This is much longer than first suggested by comparison with the deglaciation following the LGM. Despite the very high atmospheric CO_2 requested to melt the snowball Earth, the immediate post-snowball climate seems to have been not as warm and humid as previously thought. Finally, the uncertainties in evaluating the timescale of cap dolostones deposition mostly reside in our incapacity to simulate the post-snowball climate at the time of melting using the physical climate theories.

Acknowledgments

This research was supported by the Brazilian FAPESP (grants 98/03621-4 and 02/02762-0), the French CNRS program ECLIPSE and the CAPES–COFECUB cooperation program (442/4). We acknowledge

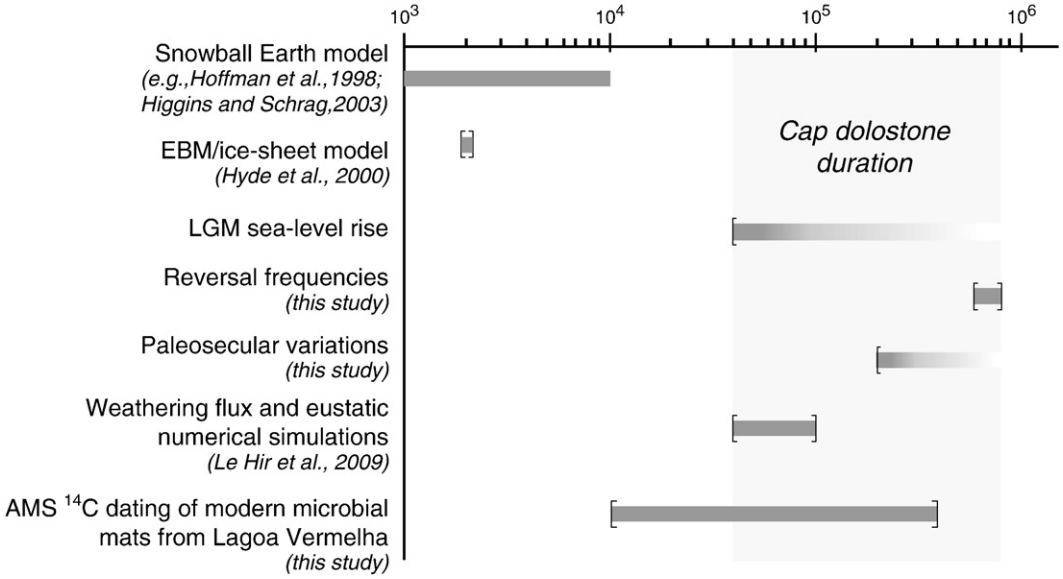

Fig. 5. Estimative of cap dolostone duration.

A. Nogueira and C. Riccomini for their important help in the stratigraphic control of the sampling in MO quarry. Particular thanks are given to Paul Hoffman for numerous discussions and for inviting E.F. to the 2008 geological excursion in Namibia. Discussions with Y. Donnadieu, G. Le Hir, C. Ritz, Y. Godderis, H. Gallée and F. Rémy are also acknowledged. The trip to Lagoa Vermelha was supported by the CAPES-COFECUB Project 442/04/06 of A.N. and R.I.F.T. We thank the contribution of J.P. Dumoulin of the Laboratoire de Mesure du Carbone 14 of Gif-sur-Yvette. ^{14}C dating was supported by the INSU-ARTEMIS program. Constructive reviews by P. Hoffman and an anonymous reviewer contributed greatly to improve the manuscript.

References

Ader, M., Macouin, M., Trindade, R.I.F., Hadrien, M.H., Yang, Z., Sun, Z., Besse, J., 2009. A multilayered water column in the Ediacaran Yangtze platform? Insights from carbonate and organic matter paired $\delta^{13}C$. Earth Planetary Science Letters 288, 213–227.

Allen, P.A., Hoffman, P.F., 2005. Extreme winds and waves in the aftermath of a Neoproterozoic glaciation. Nature 433, 123–127.

Alvarenga, C.J.S.De., Dardenne, M.A., Santos, R.V., Brod, E.R., Gioia, S.M.C.L., Sial, A.N., Dantas, E.L., Ferreira, V.P., 2007. Isotope stratigraphy of Neoproterozoic cap carbonates in the Araras Group, Brazil. Gondwana Research 13, 469–479.

Anderson, S.P., Drever, J.I., Frost, C.D., Holden, P., 2000. Chemical weathering in the foreland of a retreating glacier. Geochimica et Cosmochimica Acta 64, 1173–1189.

Babinski, M., Trindade, R.I.F., de Alvarenga, C.J.S., Boggiani, P.C., Liu, D., Santos, R.V., 2006. Geochronological constraints on the Neoproterozoic glaciations in Brazil. Snowball Earth 2006, Ascona Proceedings, v. 1, pp. 19–20.

Baker, P.A., Kastner, M., 1981. Constraints on the formation of sedimentary dolomite. Science 213, 214–216.

Bamber, J.L., Alley, R.B., Joughin, I., 2007. Rapid response of modern day ice sheets to external forcing. Earth and Planetary Science Letters 257, 1–13.

Bard, E., Hamelin, B., Fairbanks, R.G., 1990. U-Th ages obtained by mass spectrometry in corals from Barbados: sea level during the past 130, 000 years. Nature 346, 456–458.

Bard, E., Hamelin, B., Arnold, M., Montaggioni, L., Cabioch, G., Faure, G., Rougerie, F., 1996. Deglacial sea-level record from Tahiti corals and the timing of global meltwater discharge. Nature 382, 241–244.

Barton, C.E., McElhinny, M.W., 1981. A 10 000 yr geomagnetic secular variation record from three Australian maars. Geophysical Journal of the Royal Astronomical Society 67, 465–485.

Bentley, M.J., 1999. Volume of Antarctic Ice at the Last Glacial Maximum, and its impact on global sea level change. Quaternary Science Reviews 18, 1569–1595.

Bodiselitsch, B., Koeberl, C., Master, S., Reimold, W.U., 2005. Estimating duration and intensity of Neoproterozoic snowball glaciations from Ir anomalies. Science 308, 239–242.

Brachert, T.C., 1999. Non-skeletal carbonate production and stromatolite growth within a Pleistocene deep ocean (Last Glacial Maximum, Red Sea). Facies 40, 211–228.

Bullard, E.C., Freedman, C., Gellman, H., Nixon, J., 1950. The westward drift of the earth's magnetic field. Philosophical Transactions of the Royal Society of London A243, 67–92.

Burns, S.J., McKenzie, J.A., Vasconcelos, C., 2000. Dolomite formation and biogeochemical cycles in the Phanerozoic. Sedimentology 47, 49–61.

Charbit, S., Ritz, C., Ramstein, G., 2002. Simulations of Northern Hemisphere ice-sheet retreat: sensitivity to physical mechanisms involved during the Last Deglaciation. Quaternary Scinece Reviews 21, 242–265.

Clark, P.U., Mix, A.C., 2000. Global change — ice sheets by volume. Nature 406, 689–690.

Corsetti, F.A., Grotzinger, J.P., 2005. Origin and significance of tube structures in Neoproterozoic post-glacial cap carbonates: example from Noonday Dolomite, Death Valley, United States. Palaios 20, 348–363.

Corsetti, F.A., Awramik, S.M., Pierce, D.A., 2003. Complex microbiota from snowball Earth times: microfossils from the Neoproterozoic Kingston Peak Formation, Death Valley, USA. Proceedings of the National Academy of Sciences of the United States of America 100, 4399–4404.

Corsetti, F.A., Olcott, A.N., Bakermans, C., 2006. The biotic response to neoproterozoic snowball Earth. Palaeogeography, Palaeoclimatology, Palaeoecology 232, 114–130.

Cox, A., Doell, R.R., Dalrymple, G.B., 1964. Reversals of the Earth's magnetic field. Science 144, 1537–1543.

Donnadieu, Y., Fluteau, F., Ramstein, G., Ritz, C., Besse, J., 2003. Is there a conflict between the Neoproterozoic glacial deposits and the snowball Earth interpretation: an improved understanding with numerical modeling. Earth and Planetary Science Letters 208, 101–112.

Elie, M., Nogueira, A.C.R., Nédélec, A., Trindade, R.I.F., Kenig, F., 2007. A red algal bloom in the aftermath of the Marinoan Snowball Earth. Terra Nova 19, 303–308.

Font, E., Trindade, R.I.F., Nédélec, A., 2005. Detrital remnant magnetization in hematite-bearing Neoproterozoic Puga cap dolostone, Amazon Craton: a rock magnetic and SEM study. Geophysical Journal International 163, 491–500.

Font, E., Nédélec, A., Trindade, R.I.F., Macouin, M., Charrière, A., 2006a. Chemostratigraphy of the Neoproterozoic MO cap dolostones, Mato Grosso, Brazil: an alternative model for Marinoan cap dolostone formation. Earth and Planetary Science Letters 250, 89–103.

Font, E., Trindade, R.I.F., Nédélec, A., 2006b. Remagnetization in bituminous limestones of the Neoproterozoic Araras Group Amazon Craton: hydrocarbon maturation, burial diagenesis or both? Journal of Geophysical Research 111, B06204. doi:10.1029/2005JB004106.

Gaillardet, J., Dupré, B., Louvat, P., Allègre, C.J., 1999. Global silicate weathering and CO2 consumption rates deduced from the chemistry of large rivers. Chemical Geology 159, 3–30.

Gallet, Y., Courtillot, V., 1995. Geomagnetic reversal behaviour since 100 Ma. Physics of the Earth and Planetary Interiors 92, 235–244.

Gallet, Y., Pavlov, V., Courtillot, V., 2003. Magnetic reversal frequency and apparent polar wander of the Siberian platform in the earliest Palaeozoic, inferred from the Khorbusuonka river section northeastern Siberia. Geophysical Journal International 154, 829–840.

Goddéris, Y., Joachimski, M.M., 2004. Global change in the late Devonian: modelling the Frasnian–Famennian short-term carbon isotope excursions. Palaogeography, Palaeoclimatology, Palaeoecology 202, 309–329.

Goodman, J.C., Pierrehumbert, R.T., 2002. Galcial flow of floating marine ice in "Snowball earth". Journal of Geophysical Research 108, C10. doi:10.1029/2002JC001471.

Goodsite, M.E., Rom, W., Heinemeier, J., Lange, T., Ooi, S., Appleby, P.G., Shotyk, W., van der Knaap, W.O., Lohse, C., Hansen, T.S., 2001. High -resolution AMS C-14 dating of post-bomb peat archives of atmospheric pollutants. Radiocarbon 43, 495–515.

Grassineau, N.V., Nisbet, E.G., Fowler, C.M.R., Bickle, M.J., Lowry, D., Chapman, H.J., Mattey, D.P., Abell, D.P., Yong, J., Martin, A., 2002. Stable isotopes in the Archaean Belingwe belt, Zimbabwe: evidence for a diverse microbial mat ecology. Journal of the Geological Society of London 199, 309–328.

Grotzinger, J.P., Knoll, A.H., 1999. Stromatolites in Precambrian carbonates: evolutionary mileposts or environmental dipsticks? Annual Review of Earth and Planetary Sciences 27, 313–358.

Gubbins, D., 1999. The distinction between geomagnetic excursions and reversals. Geophysical Journal International 137, F1–F3.

Halverson, G.P., Dudas, F.Ö., Maloof, A.C., Bowring, A.S., 2007. Evolution of the $^{87}Sr/^{86}Sr$ composition of Neoproterozoic seawater. Palaeogeography, Palaeoclimatology, Palaeoecology 256, 103–129.

Higgins, J.A., Schrag, D.P., 2003. Aftermath of a snowball Earth. Geochemistry, Geophysics, Geosystems 4, 1–20.

Hoffman, P.F., Li, Z.X., 2009. A palaeogeographic context for Neoproterozoic glaciation. Palaeogeography, Palaeoclimatology, Palaeoecology 277, 158–172.

Hoffman, P.F., Schrag, D.P., 2002. The snowball Earth hypothesis: testing the limits of global change. Terra Nova 14, 129–155.

Hoffman, P.F., Kaufman, A.J., Halverson, G.P., Schrag, D.P., 1998. A Neoproterozoic snowball Earth. Science 281, 1342–1346.

Hoffman, P.F., Halverson, G.P., Domack, E.W., Husson, J.M., Higgins, J.A., Shrag, D.P., 2007. Are basal Ediacaran 635 Ma post-glacial « cap dolostones » diachronous? Earth and Planetary Science Letters 258, 114–131.

Huybrechts, P., 2002. Sea-level changes at the LGM from ice-dynamic reconstructions of the Greenland and Antarctic ice sheets during the glacial cycles. Quaternary Science Reviews 21, 203–231.

Hyde, W.T., Crowley, T.J., Baum, S.K., Peltier, W.R., 2000. Neoproterozoic 'snowball Earth' simulations with a coupled climate/ice-sheet model. Nature 405, 425–429.

Jiang, G., Christie-Blick, N., Kaufman, A.J., Banerjee, D.M., Rai, V., 2003. Carbonate platform growth and cyclicity at a terminal Proterozoic passive margin, Infra Krol Formation and Krol Group, Lesser Himalaya, India. Sedimentology 50, 921–952.

Kasemann, S.A., Hawkesworth, C.J., Prave, A.R., Fallick, A.E., Pearson, P.N., 2005. Boron and calcium isotope composition in Neoproterozoic carbonate rocks from Namibia: evidence for extreme environmental change. Earth and Planetary Science Letters 231, 73–86.

Kaufman, A.J., Knoll, A.H., Narbonne, G.M., 1997. Isotopes, ice ages, and terminal Proterozoic Earth history. Geology 94, 6600–6605.

Kennedy, M.J., 1996. Stratigraphy, sedimentology, and isotope geochemistry of Australian Neoproterozoic glacial cap dolostones: deglaciation, $\delta^{13}C$ excursions, and carbonate precipitation. Journal of Sedimentary Research 66, 1050–1064.

Kennedy, M.J., Christie-Blick, N., Sohl, L.E., 2001. Are Proterozoic cap carbonates and isotopic excursions a record of gas hydrate destabilization following Earth's coldest intervals? Geology 29, 443–446.

Kilner, B., McNiocaill, C., Brasier, M., 2005. Low-latitude in the Neoproterozoic of Oman. Geology 33, 413–416.

Kirschvink, J.L., 1979. A paleomagnetic approach to the Precambrian boundary problem. Unpublished Ph.D thesis, Princeton University.

Kirschvink, J.L., 1992. Late Proterozoic low-latitude global glaciation: the snowball Earth, dans. In: Schopf, J.W., Klein, C. (Eds.), The Proterozoic Biosphere. Cambridge University Press, pp. 51–52.

Lambeck, K., Yokoyama, Y., Johnston, P., Purcell, A., 2000. Global ice volumes at the Last Glacial Maximum and early Lateglacial. Earth and Planetary Sciences Letters 181, 513–527.

Land, L.S., 1998. Failure to precipitate dolomite at 25 degrees C from dilute solution despite 1000-fold oversaturation after 32 years. Aquatic Geochemistry 4, 361–368.

Le Hir, G., Donnadieu, Y., Goddéris, Y., Pierrehumbert, R.T., Halverson, G.P., Macouin, M., Nédélec, A., Ramstein, G., 2009. The Snowball Earth aftermath: exploring the limits of continental weathering processes. Earth and Planetary Science Letters 277, 453–463.

Li, Z.X., 2000. New paleomagnetic results from the 'cap dolomite' of the Neoproterozoic Walsh Tillite, northwestern Australia. Precambrian Research 100, 359–370.

Mackereth, F.J.H., 1971. On the variation in the direction of the horizontal component in lake sediments. Earth and Planetary Science Letters 12, 332–338.

Marshall, W.A., Gehrels, W.R., Garnett, M.H., Freeman, S.P.H.T., Maden, C., Xu, S., 2007. The use of 'bomb spike' calibration and high-precision AMS 14C analyses to date salt-marsh sediments deposited during the past three centuries. Quaternary Research 68, 325–337.

Matuyama, M., 1929. On the direction of magnetization of basalt in Japan, Tyosen and Manchuria. Proceedings of the Imperial Academy of Japan 5, 203–205.
McFadden, P., McElhinny, M.W., 1990. Classification of the reversal test in paleomagnetism. Geophysical Journal International 103, 725–729.
Mercanton, P.I., 1926. Inversion de l'inclinaison magnétique terrestres aux âges géologiques. Terrestrial Magnetism and Atmospheric Electricity 31, 187–190.
Merrill, R.T., McElhinny, M.W., McFadden, P.L., 1996. The magnetic field of the earth — paleomagnetism, the core, and the deep mantle. Academic Press, San Diego, California.
Mook, W.G., van der Plicht, J., 1999. Reporting C-14 activities and concentrations. Radiocarbon 41, 227–239.
Nédélec, A., Affaton, P., France-Lanord, C., Charrière, A., Alvaro, J., 2007. Sedimentology and chemostratigraphy of the Bwipe Neoproterozoic cap dolostones Ghana, Volta Basin: a record of microbial activity in a peritidal environment. Comptes Rendus Geoscience 339, 223–239.
Nogueira, A.C.R., Riccomini, C., Sial, A.N., Moura, C.A.V., Fairchild, T.R., 2003. Soft-sediment deformation at the base of the Neoproterozoic Puga cap carbonate southwestern Amazon Craton, Brazil: confirmation of rapid icehouse-greenhouse transition in snowball earth. Geology 31, 613–616.
Nogueira, A.C.R., Riccomini, C., Sial, A.N., Moura, C.A.V., Trindade, R.I.F., Fairchild, T.R., 2007. S and Sr isotope fluctuations and paleoceanographic changes in the late Neoproterozoic Araras carbonate platform, southern Amazon craton, Brazil. Chemical Geology 237, 168–190.
Olcott, A.N., Session, A.L., Corsetti, F.A., Kaufman, A.J., de Oliviera, T.F., 2005. Biomarker evidence for photosynthesis during Neoproterozoic glaciation. Science 310, 471–474.
Pavlov, V., Gallet, Y., 2001. Middle Cambrian high magetic reversal frequency Kulumbe River section, northwestern Siberia and reversal behaviour during the Early Palaeozoic. Earth and Planetary Science Letters 185, 173–183.
Peltier, W.R., Fairbanks, R.G., 2006. Quaternary Science Reviews 25, 3322–3337.
Pierrehumbert, R.T., 2004. High levels of atmospheric carbon dioxyde necessary for the termination of global glaciation. Nature 429, 646–649.
Pollard, D., Kasting, J.F., 2005. Snowball Earth: a thin-ice solution with flowing seaglaciers. Journal of Geophysical Research 110, C0710. doi:10.1029/2004JC002525.
Raub, T.D., Evans, D.A.D., 2005. Magnetostratigraphy of the type-marinoan succession and correlatives throughout Australia. Salt Lake City Annual Meeting of Geological Survey of American Bulletin.
Reid, R.P., Visscher, P.T., Decho, A.W., Stolz, J.F., Bebout, B.M., Dupraz, C., Macintyre, I.G., Paerl, H.W., Pinckney, J.L., Prufert-Bebout, L., Steppe, T.F., Desmarais, D.J., 2000. The role of microbes in accretion, lamination and early lithification of modern marine stromatolites. Nature 406, 989–992.
Rieu, R., Allen, P.A., Plötze, M., Pettke, T., 2007a. Compositional and mineralogical variations in a Neoproterozoic glacially influenced succession, Mirbat area, south Oman: implications for paleoweathering conditions. Precambrian Research 154, 248–265.
Rieu, R., Allen, P.A., Plötze, M., Pettke, T., 2007b. Climatic cycles during a Neoproterozoic "snowball" glacial epoch. Geology 35, 299–302.
Smith, G., Creer, K.M., 1986. Analysis of geomagnetic secular variation 10,000 to 30,000 years BP, Lac-du-Bouchet, France. Physics of the Earth and Planetary Interiors 44, 1–14.
Sohl, L.E., Christie-Blick, N., Kent, D.V., 1999. Paleomagnetic polarity reversals in Marinoan ca. 600 Ma glacial deposits of Australia: implications for the duration of low-latitude glaciations in Neoproterozoic time. Geological Society of American Bulletin 111, 1120–1139.
Thouveny, N., Williamson, D., 1988. Paleomagnetic study of the holocene and upper pleistocene sediments from lake Barombi Mbo, Cameroun — 1st results. Physics of the Earth and Planetary Interiors 52, 193–206.
Thouveny, N., Creer, K.M., Blunk, I., 1990. Extension of the Lac du Bouchet palaeomagnetic record over the last 120,000 years. Earth and Planetary Science Letters 97, 140–161.
Trindade, R.I.F., Macouin, M., 2007. Paleolatitude of glacial deposits and paleogeography of Neoproterozoic ice ages. Comptes Rendus Geoscience 339, 200–211.
Trindade, R.I.F., Font, E., D'Agrella-Filho, M.S., Nogueira, A.C.R., Riccomini, C., 2003. Low-latitude and multiple geomagnetic reversals in the Neoproterozoic Puga cap carbonates. Terra Nova 15, 441–446.
Turetsky, M.R., Manning, S.W., Wieder, R.K., 2004. Dating recent peat deposits. Wetlands 24, 324–356.
van Lith, Y., Warthmann, R., Vasconcelos, C., McKenzie, J., 2003a. Microbial fossilization in carbonate sediments: a result of the bacterial surface involvement in dolomite precipitation. Sedimentology 50, 237–245.
van Lith, Y., Warthmann, R., Vasconcelos, C., McKenzie, J., 2003b. Sulphate-reducing bacteria induce low-temperature Ca-dolomite and high Mg-calcite formation. Geobiology 1, 71–79.
Vasconcelos, C., McKenzie, J.A., 1997. Microbial mediation of modern dolomite precipitation and diagenesis under anoxic conditions Lagoa Vermelha, Rio de janeiro, Brazil. Journal of Sedimentary Research A67, 378–390.
Vasconcelos, C., Warthmann, R., McKenzie, J., Visscher, P.T., Bittermann, A.G., van Lith, Y., 2006. Lithifying microbial mats in Lagoa Vermelha, Brazil: modern Precambrian relics? Sedimentary Geology 185, 175–183.
Vincent, W.F., Howard-Williams, C., 2000. Life on snowball Earth. Science 287, 2421.
Warren, J., 2000. Dolomite: occurrence, evolution and economically important associations. Earth Science Reviews 52, 1–81.
Warren, S.G., Brandt, R.E., Grenfell, T.C., McKay, C.P., 2002. Snowball Earth: ice thickness on the tropical ocean. Journal of Geophysical Research 107, C10. doi:10.1029/2001JC001123.
Wicht, J., Olson, P., 2004. A detailed study of the polarity reversal mechanism in a numerical dynamo model. Geochemistry Geophysics Geosystems 5. doi:10.1029/2003GC000602.